

Received:  
3 October 2017  
Revised:  
9 March 2018  
Accepted:  
11 April 2018

Cite as: Fabian Lohöfer,  
Laura Hoffmann,  
Rebecca Buchholz,  
Katharina Huber,  
Almut Glinzer,  
Katja Kosanke, Annette  
Feuchtinger,  
Michaela Aichler,  
Benedikt Feurecker,  
Georgios Kaissis,  
Ernst J. Rummeny,  
Carsten Höltnke,  
Cornelius Faber,  
Franz Schilling,  
René M. Botnar,  
Axel K. Walch, Uwe Karst,  
Moritz Wildgruber. Molecular  
imaging of myocardial  
infarction with Gadofluorine P  
– A combined magnetic  
resonance and mass  
spectrometry imaging  
approach.  
Heliyon 4 (2018) e00606.  
doi: 10.1016/j.heliyon.2018.  
e00606



# Molecular imaging of myocardial infarction with Gadofluorine P – A combined magnetic resonance and mass spectrometry imaging approach

Fabian Lohöfer<sup>a</sup>, Laura Hoffmann<sup>a</sup>, Rebecca Buchholz<sup>b</sup>, Katharina Huber<sup>c</sup>,  
Almut Glinzer<sup>a</sup>, Katja Kosanke<sup>a</sup>, Annette Feuchtinger<sup>c</sup>, Michaela Aichler<sup>c</sup>,  
Benedikt Feurecker<sup>d</sup>, Georgios Kaissis<sup>a</sup>, Ernst J. Rummeny<sup>a</sup>, Carsten Höltnke<sup>e</sup>,  
Cornelius Faber<sup>e</sup>, Franz Schilling<sup>d</sup>, René M. Botnar<sup>f</sup>, Axel K. Walch<sup>c</sup>, Uwe Karst<sup>b</sup>,  
Moritz Wildgruber<sup>a,e,\*</sup>

<sup>a</sup> Department of Diagnostic and Interventional Radiology, Klinikum Rechts der Isar, Technische Universität München, Munich, Germany

<sup>b</sup> Department of Analytical Chemistry, Westfälische Wilhelms Universität, Münster, Germany

<sup>c</sup> Germany Research Unit Analytical Pathology, Institute of Pathology, Helmholtz Zentrum München, Oberschleißheim, Germany

<sup>d</sup> Department of Nuclear Medicine, Klinikum Rechts der Isar, Technische Universität München, Munich, Germany

<sup>e</sup> Translational Research Imaging Center, Department of Clinical Radiology, University Hospital Münster, Münster, Germany

<sup>f</sup> Division of Imaging Sciences and Biomedical Engineering, King's College London, London, United Kingdom

\* Corresponding author.

E-mail address: [moritz.wildgruber@ukmuenster.de](mailto:moritz.wildgruber@ukmuenster.de) (M. Wildgruber).

## Abstract

**Background:** Molecular MRI is becoming increasingly important for preclinical research. Validation of targeted gadolinium probes in tissue however has been cumbersome up to now. Novel methodology to assess gadolinium distribution in tissue after in vivo application is therefore needed.

**Purpose:** To establish combined Magnetic Resonance Imaging (MRI) and Mass Spectrometry Imaging (MSI) for improved detection and quantification of Gadofluorine P deposition in scar formation and myocardial remodeling.

**Materials and methods:** Animal studies were performed according to institutionally approved protocols. Myocardial infarction was induced by permanent ligation of the left ascending artery (LAD) in C57BL/6J mice. MRI was performed at 7T at 1 week and 6 weeks after myocardial infarction. Gadofluorine P was used for dynamic  $T_1$  mapping of extracellular matrix synthesis during myocardial healing and compared to Gd-DTPA. After in vivo imaging contrast agent concentration as well as distribution in tissue were validated and quantified by spatially resolved Matrix-Assisted Laser Desorption Ionization (MALDI) MSI and Laser Ablation – Inductively Coupled Plasma – Mass Spectrometry (LA-ICP-MS) imaging.

**Results:** Both Gadofluorine P enhancement as well as local tissue content in the myocardial scar were highest at 15 minutes post injection.  $R_1$  values increased from 1 to 6 weeks after MI ( $1.62 \text{ s}^{-1}$  vs  $2.68 \text{ s}^{-1}$ ,  $p = 0.059$ ) paralleled by an increase in Gadofluorine P concentration in the infarct from 0.019 mM at 1 week to 0.028 mM at 6 weeks ( $p = 0.048$ ), whereas Gd-DTPA enhancement showed no differences ( $3.95 \text{ s}^{-1}$  vs  $3.47 \text{ s}^{-1}$ ,  $p = 0.701$ ). MALDI-MSI results were corroborated by elemental LA-ICP-MS of Gadolinium in healthy and infarcted myocardium. Histology confirmed increased extracellular matrix synthesis at 6 weeks compared to 1 week.

**Conclusion:** Adding quantitative MSI to MR imaging enables a quantitative validation of Gadofluorine P distribution in the heart after MI for molecular imaging.

Keywords: Biomedical engineering, Cardiology, Medical imaging

## 1. Introduction

Following ischemia, the left ventricular myocardium undergoes a series of changes in geometry, function and biochemical adaptations. A collagen-rich extracellular matrix is produced to replace lost cardiomyocytes in the infarct to form a stable scar [1]. Successful infarct healing requires a balance between synthesis and degradation of extracellular matrix to preserve cardiovascular function. Excessive extracellular matrix (ECM) formation, both in the infarcted but also in the remote myocardium, can result in increased wall stiffness and decline of compliance, subsequently leading to diastolic dysfunction [2]. On the other hand, insufficient production of extracellular matrix components can lead to progressive thinning of the myocardial wall and expansion of the infarcted area, with increased risk for left

ventricular dilatation with progressive heart failure [3], aneurysm formation or even rupture [4, 5].

To better visualize ECM synthesis during myocardial healing and remodeling, more specific and quantitative imaging methods are desirable. With the advent of molecular contrast agents that bind to specific extracellular matrix proteins such as collagen [6, 7] or elastin [8], imaging of ECM remodeling has become feasible. Until recently MRI was only used to generate weighted images (e.g. T1-weighting or T2-weighting), which are not quantitative. T1 mapping, currently the most accurate tool to quantify accumulation of gadolinium agents, provides reliable assessment of gadolinium induced relaxation rate changes [9]. However, the imaging signal itself may not directly correlate with the actual amount of the molecular gadolinium probe in tissue, as the signal is influenced by a variety of additional factors of the local microenvironment such as pH-levels, oxygenation, extra- and intracellular compartmentalization of the gadolinium molecules [10, 11]. Spatially-resolved quantification of gadolinium agents in tissue has not been possible until recently. Matrix Assisted Laser Desorption Ionization - Mass Spectrometry Imaging (MALDI-MSI) can be used to visualize and precisely quantify various gadolinium chelates in tissue sections after the contrast agent has been applied *in vivo* [12]. Laser Ablation – Inductively Coupled Plasma – Mass Spectrometry (LA-ICP-MS) imaging can achieve quantitative resolution of gadolinium molecules in tissue almost at cellular resolution [13].

In the current study, we aim to combine MRI and MSI in a multiscale imaging approach to quantitatively track Gadofluorine P accumulation as a surrogate for ECM concentration during myocardial healing and remodeling. We hypothesize that Gadofluorine P would enable us to follow the process of ECM deposition in the infarct zone after experimental myocardial infarction, and that MSI provides complementary spatial and quantitative information for molecular contrast agent deposition.

## 2. Materials and methods

### 2.1. Animal model

Myocardial infarction (MI) was performed in female C57BL/6J mice (aged 10–14 weeks, Charles River Laboratories, Sulzfeld, Germany) by permanent ligation of the left anterior descending artery (LAD) as previously described [8]. MR kinetic studies applying T1 mapping were performed in  $n = 7$  mice per time point for Gadofluorine P and Gd-DTPA as reference. The kinetic study for Gd-DTPA was performed over 120 minutes. After administration of Gadofluorine P an additional measurement after 12 hours was performed due to the extended kinetic profile. For the assessment of extracellular matrix (ECM) synthesis over time MR imaging was performed either at 1 week and mice were sacrificed thereafter or at 1 and 6 weeks after myocardial

infarction with subsequent sample preparation for MSI and histology. For assessment of the Gadofluorine P concentration kinetics by MSI infarcted mice were investigated at 6 weeks post MI and animals were sacrificed at 8 min, 15 min, 21 min, 30 min, 40 min and 60 min after injection of the contrast agent. All animal experiments were approved by the local subcommittee on Research Animal Care (Protocol Number 55.2-1-54-2532-85-13).

## 2.2. Contrast agents

Gadofluorine P is a further derivative of Gadofluorine M (Bayer Healthcare, Berlin, Germany), an amphiphilic experimental MRI contrast agent, composed of a Gd-DO3A derivative with a lysine linker, a hydrophilic sugar moiety (mannose) and a perfluorinated lipophilic side chain, which has been shown to bind to collagen, proteoglycans and tenascin in animal models of atherosclerosis [14]. The binding towards extracellular matrix proteins is mainly due to an unspecific adsorption towards proteins and filaments resulting from different charge properties. Due to the prolonged blood and tissue half-life and subsequent delayed excretion, Gadofluorine M has been discontinued and modified by replacing the lysine backbone with a shorter ethylenediamine linker and the sugar moiety by a short polyethyleneglycol unit, leading to the generation of Gadofluorine P (invivoContrast GmbH, Berlin, Germany). Chemical structure and mass spectrum showing the respective  $m/z$  at 1323.2 Da with the Gadolinium specific isotope pattern is shown in Fig. 1. Gadofluorine P is an amphiphilic, iso-osmolar gadolinium agent with a plasma protein binding of more than 90%, resulting in a plasma half-life in rats of about 2 hours. Gadopentetate dimeglumine (Gd-DTPA, Bayer Healthcare, Berlin, Germany) was used as an unspecific reference agent.

## 2.3. MR imaging

Magnetic Resonance Imaging was performed on a horizontal bore 7T small animal scanner (Discovery MR901, GE Healthcare, Chalfont St. Giles, United Kingdom)

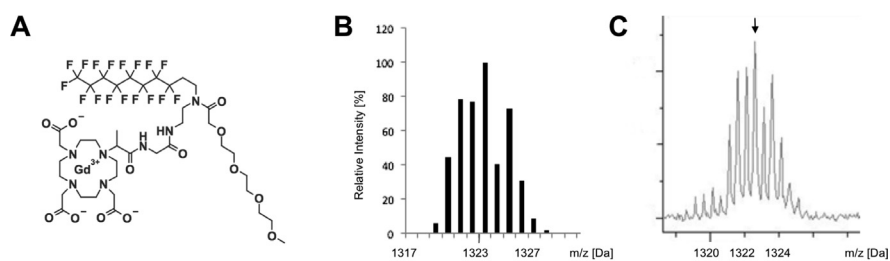


**Fig. 1.** Chemical structure and Mass spectrum of Gadofluorine P. Chemical structure (A) and predicted isotope pattern of Gadofluorine P (B). For peak identification, the mass spectra obtained from heart sections (C) were compared to the predicted isotope distribution pattern.

equipped with a  $300 \text{ mTm}^{-1}$  standard high-field gradient system and a 72 mm inner diameter  $^1\text{H}/^{13}\text{C}$  quadrature birdcage resonator (Rapid Biomedical, Rimpar, Germany). Image acquisition was performed under free-breathing conditions and prospective ECG triggering (Rapid Biomedical, Rimpar, Germany). During imaging, the animals' temperature was maintained at  $\approx 38^\circ\text{C}$  using an MR-compatible heating system (Bruker Biospin, Ettlingen, Germany).

Both contrast agents were injected at a dose of  $0.2 \text{ mmol kg}^{-1}$  body weight via the tail vein. After determining a peak enhancement of Gadofluorine P within the myocardial scar at a time point of 15 minutes, imaging for subsequent experiments was then routinely performed at 15 minutes after contrast agent injection. All scans were acquired as short axis views. On the 3-plane scout scans a long axis scan was planned as a first step. In a second step a 4-chamber view was acquired. The short axis views were planned perpendicular to the long axis view and 4-chamber view. After selecting short-axis planes for Late gadolinium enhancement (LGE) assessment, a segmented inversion-recovery fast gradient echo sequence was performed using the following parameters: FOV  $30 \times 30 \text{ mm}$ , matrix  $192 \times 192$  (in-plane resolution  $156 \mu\text{m}$ ), slice thickness 1 mm, TR/TE/TI 7.6 ms/3.1 ms/350 ms, flip angle  $60^\circ$ , 4 k-space lines/RR interval, 2 scans, and 8 slices. After delayed enhancement acquisition single-slice T1 mapping was performed in the same geometry in one midventricular short axis slice with the largest extent of the infarcted myocardium on LGE imaging. A standard inversion prepared prospectively ECG-gated Look-Locker sequence was used. Specific sequence parameters were as followed: FOV  $30 \times 30 \text{ mm}$ , matrix  $128 \times 128$  (in-plane resolution  $234 \mu\text{m}$ ), slice thickness 1 mm, TR/TE 5.1 ms/1.3 ms, flip angle  $8^\circ$ , 4 lines/RR interval, 2 scans, total scan time ca. 8 min. For T1 estimation, Look-Locker data analysis was performed using an open-source software tool (MRmap v1.4) for the generation of relaxation time maps in MRI [15]. T1 images were calculated from DICOM source images based on a 3-parameter Levenberg-Marquardt curve fitting procedure with a correction for read-out-induced attenuation of the relaxation curve as described previously [16]. Regions of interest (ROI) were drawn manually in the in the infarcted myocardium and remote myocardium based on the LGE images and then copied to the T1 maps.

Cardiac function was determined by established CINE imaging. CINE images for the assessment of cardiac function were acquired as a stack of 8 slices in the short axis plane to cover the entire left ventricle. The CINE images were acquired in each animal before the administration of the contrast agent. CINE acquisition was synchronized with every R wave. Sequence parameters were: FOV  $30 \times 30 \text{ mm}$ , matrix  $128 \times 128$  (in-plane resolution  $234 \mu\text{m}$ ), slice thickness 1 mm, TR/TE 2.77 ms/0.86 ms, flip angle  $30^\circ$ , 4 scans. An average of 12 cardiac cycles was acquired per slice. The ejection fraction was calculated from CINE images as followed:  $[(\text{End diastolic volume} - \text{End systolic volume})/\text{End diastolic volume}] \times 100$ .

## 2.4. MALDI-MSI and histology

MALDI combines extraction of molecules of interest via an overlying matrix with a time of flight approach to analyze ionized molecules depending on their mass, respectively charge they generate once reaching the detector. The advantage of MALDI is that the sample itself is not ablated, as it is the case with LA-ICP-MS, and can thus be used further for histology/immunohistochemistry. Sectioning of fresh frozen infarcted mouse hearts was performed as described previously [12]. Cryosections (12  $\mu\text{m}$  thickness) were prepared and mounted onto conductive Indium-Tin-Oxide (ITO) glass slides (Bruker Daltonik GmbH, Bremen, Germany), which were pre-coated with 1:1 poly-L-lysine (Sigma-Aldrich, Taufkirchen, Germany) and 0.1 % Nonidet P-40 (nonylphenoxy polyethoxy ethanol 40, Sigma-Aldrich, Taufkirchen, Germany). Detection of Gadofluorine P was optimized as described previously. For quantification of Gadofluorine P signal, a standard curve was prepared additionally for each slide. For this purpose, liver cryosections of untreated mice were mounted on the ITO slides and 0.5  $\mu\text{l}$  Gadofluorine P, diluted in water to concentrations ranging from 0.5 to 0.01 mg/ml (0.3782 mM–0.0076 mM), was spotted onto the liver sections. To obtain digital images for co-registration, heart sections were dried at room temperature and scanned using a flatbed scanner. Matrix solution, composed of 7 g/l CHCA (Sigma-Aldrich, Taufkirchen, Germany) in 70% methanol and 0.2% trifluoroacetic acid (TFA, Applied Biosystems, Darmstadt, Germany) was applied using an ImagePrep spray device (Bruker Daltonik GmbH, Bremen, Germany). MALDI-TOF Imaging measurements were carried out at a spatial resolution of 70  $\mu\text{m}$  using an Ultraflex III MALDI TOF mass spectrometer (Bruker Daltonik GmbH, Bremen, Germany) in positive reflector mode with a sampling rate of 1.0 GS/s. A total of 200 laser shots were accumulated for each position measured.

After mass spectrometry measurements, the matrix was removed with 70% ethanol and the sections were stained with an Elastica van Gieson stain (Morphisto GmbH, Frankfurt am Main, Germany). Elastica van Gieson staining was applied to stain for elastic fibers and collagen fibers. Specifically, the tissue is first stained with a Resorcin-Fuchsin-solution (also known as Weigert staining). Subsequently tissue is stained with hematoxylin and after that counterstained with picrofucsin. Cell nuclei appear as –brown-black, elastic fibers black-purple. Picrofucsin staining adds a yellow-brown staining to the cytoplasm and red stain of the collagenous fibers. All stained slides were scanned at 20x objective magnification using a Mirax Desk digital slide scanner (Carl Zeiss MicroImaging, Munich, Germany). For each of the resulting digital slides, subsets (regions of interest) were defined from areas of myocardial infarction and analyzed using commercially available software (Definiens Enterprise Image Intelligence Suite, Definiens AG, Munich, Germany). A specific rule set was developed to detect and quantify the Elastica-van-Gieson stained elastic fibers and whitespaces within the tissue based on staining intensity,

morphology, neighborhood, and special color features. The relative areas of the whitespace in comparison to the total tissue area and the relative red staining intensities of the elastic fibers were calculated. Images were subsequently merged with the mass spectrometry datasets. Data are presented as mean peak intensity.

## 2.5. Laser ablation – inductively coupled plasma – mass spectrometry (LA-ICP-MS)

While MALDI MSI is dependent on the overlying matrix and can only reach a spatial resolution of  $\sim 50 \mu\text{m}$ , LA-ICP-MS does not require an overlying matrix to extract molecules of interest and reaches a spatial resolution below  $5 \mu\text{m}$  - in the cellular range. For analysis via LA-ICP-MS, cryosections ( $10 \mu\text{m}$  thickness) were prepared with a cryomicrotome model CRYOSTAR NX70 (ThermoFisher Scientific, Bremen, Germany) using TissueTek<sup>®</sup> for fixation and were mounted onto glass slides (VWR, Darmstadt, Germany). For quantification, matrix-matched standards based on gelatin (GRÜSSING GmbH, Filsum, Germany) were prepared by mixing 100 mg gelatin with 900  $\mu\text{L}$  of Gd solutions ranging from 1 to 750 mg/L. These matrix-matched standards were homogenized at  $60 \text{ }^\circ\text{C}$  and  $10 \mu\text{m}$  cryosections were prepared.

To determine the Gd concentration of these standards, ICP-MS analysis was performed. Therefore, 50 mg of gelatin standard were dissolved in 2%  $\text{HNO}_3$  and diluted to final concentrations ranging between 1 and 30  $\mu\text{g/L}$ . All solutions contained 1  $\mu\text{g/L}$  Ho (1000 mg/L Ho, SCP Science, Quebec, Canada) as internal standard. Six Gadolinium standards ranging from 5 to 30  $\mu\text{g/L}$ , prepared from ICP standard (1000 mg/L Gd, Sigma-Aldrich, Taufkirchen, Germany) were used to quantify the dissolved gelatin standards. The analyses were performed using an ICP-MS instrument model iCAP<sup>™</sup> Q (ThermoFisher Scientific, Bremen, Deutschland) equipped with an ASX-560 autosampler, PFA Micro-Flow nebulizer, cyclonic spray chamber, Ni sampler and Ni Skimmer.

Elemental imaging with LA-ICP-MS was performed with an ICP-MS instrument model iCAP<sup>™</sup> TQ (ThermoFisher Scientific, Bremen, Deutschland) with  $\text{O}_2$  as reaction gas. Dwell times for the Gd isotopes between 0.07 and 0.1 s were used. The samples were introduced with an LSX-213 G2<sup>+</sup> laser ablation system (Teledyne CETAC, Thousand Oaks, USA) including a HelEx II ablation cell and Helium as transport gas.

The samples were ablated with a spot size between 15 and  $40 \mu\text{m}$  and an adjusted scan speed between 45 and  $120 \mu\text{m/s}$ . Nine lines per gelatin standard were ablated with the same parameters and the averaged intensities were used to quantify the Gd content via external calibration. The isotope  $^{158}\text{Gd}$  was used for quantification.

## 2.6. Statistics

Values are presented as mean  $\pm$  standard deviation (SD) or dot plot diagrams with mean and 95% confidence interval. Comparison of measurements over time between different groups were performed using 2-way analysis of variance (ANOVA) followed by Bonferroni post-hoc test for multiple comparisons. Comparison of values obtained at one versus six weeks were performed using an unpaired student's t-test (two-tailed). Comparison of  $R_1$  values with LVEF was performed using Pearson's correlation. A p-value of  $<0.05$  was considered statistically significant.

An overview of the experiments with the according sample sizes is provided in Fig. 2.

## 3. Results

### 3.1. Enhancement kinetics of Gadofluorine P compared to Gd-DTPA

To evaluate the time course of Gadofluorine P performance, a kinetic analysis of contrast enhancement for Gd-DTPA and Gadofluorine P was performed in the infarcted myocardium over time. Imaging was performed at week 6 post infarction

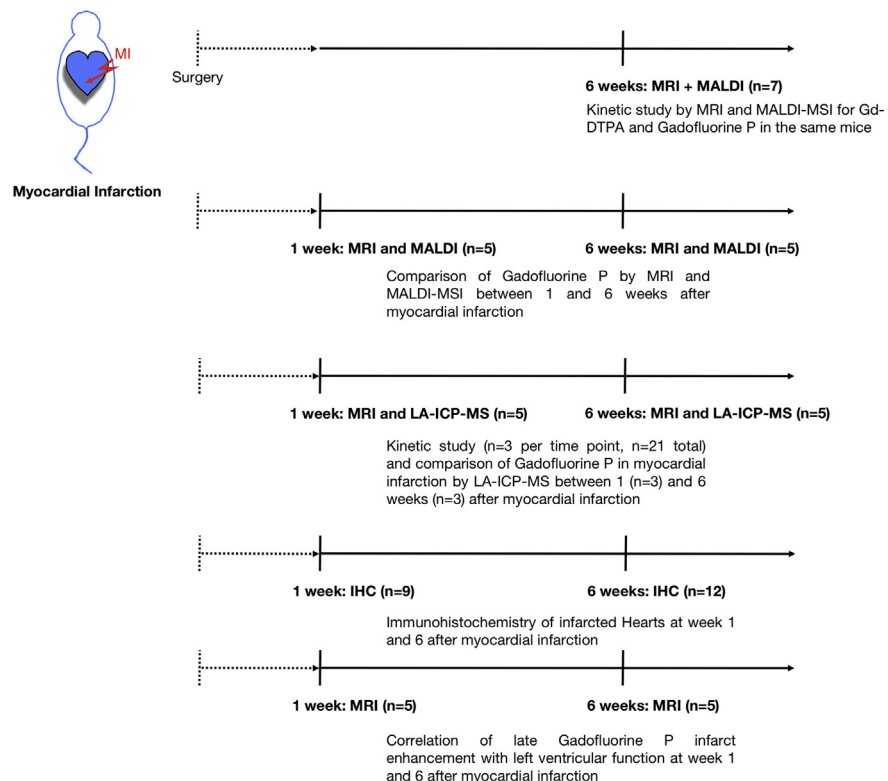


**Fig. 2.** Experimental overview. Course of experiments is provided together with the corresponding sample size, respectively mice used for each experiment.



surgery. Gadofluorine P showed highest  $R_1$  values in the infarcted myocardium at 15–20 minutes after injection and  $R_1$  values returned close to baseline at 100 minutes post injection. Highest  $R_1$  values were obtained within the blood, which is attributed to the albumin binding capacity of Gadofluorine P (Fig. 3).

### 3.2. MALDI-MSI

Gadofluorine P was successfully visualized by MALDI-MSI and the contrast agent concentrations could be mapped onto the corresponding histology sections. Gadofluorine P accumulated specifically within the infarct scar, whereas in the remote myocardium only a fraction was detectable which was localized in the myocardial vasculature (Fig. 4). Mean Gadofluorine P concentration in the infarcted myocardium peaked 15 minutes after i.v. injection (0,0224 mM). After 60 minutes the concentration in the infarcted myocardium reached the baseline (0,0069 mg/ml). The concentration in remote myocardium was constant over the whole time period (0,0069 mM 15 min p.i. to 0,0062 mM 60 min p.i.).

### 3.3. Gadofluorine P for assessment of postinfarction scar formation

To evaluate the use of our multiscale imaging approach for studying myocardial healing and remodeling, we scanned the same mice at 1 and 6 weeks after LAD ligation using Gadofluorine P-enhanced MRI and sacrificed mice at each time point for MALDI-MSI. Reference Gd-DTPA measurements showed no significant differences between  $R_1$  values in the infarcted myocardium at 1 ( $3.95 \pm 1.5 \text{ s}^{-1}$ ) and 6 ( $3.47 \pm 2.26 \text{ s}^{-1}$ ) weeks

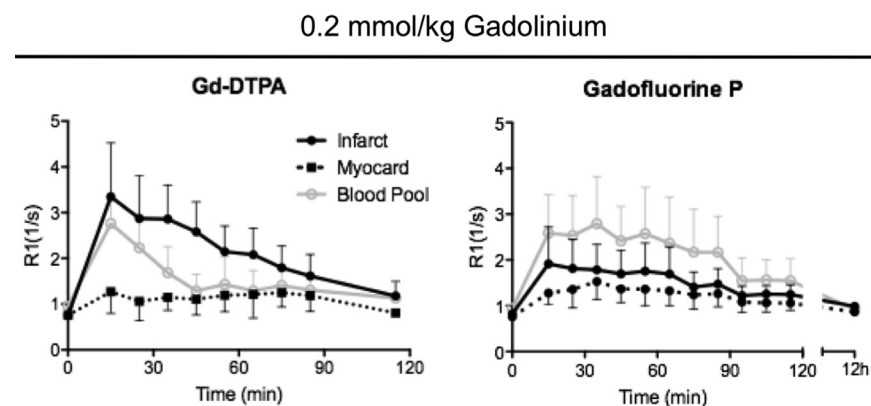


**Fig. 3.** Enhancement Kinetics after administration of contrast agents. In vivo MRI kinetic studies of contrast enhancement show  $R_1$  values after intravenous Gd-DTPA (left panel), and Gadofluorine P (right panel) administration at a concentration of 0.2 mmol/kg body weight in the same mice ( $n = 7$ ). Measurements with Gadofluorine P were performed 24h after the measurements with Gd-DTPA.  $R_1$  values are given for the area of myocardial infarction (Infarct), remote myocardium (Myocardium) and blood (Blood Pool). Mean values and SD for infarcted (+SD) and health myocardium (-SD) are shown. Gadofluorine P shows stable enhancement of the infarct scar for 15–40 minutes post injection.

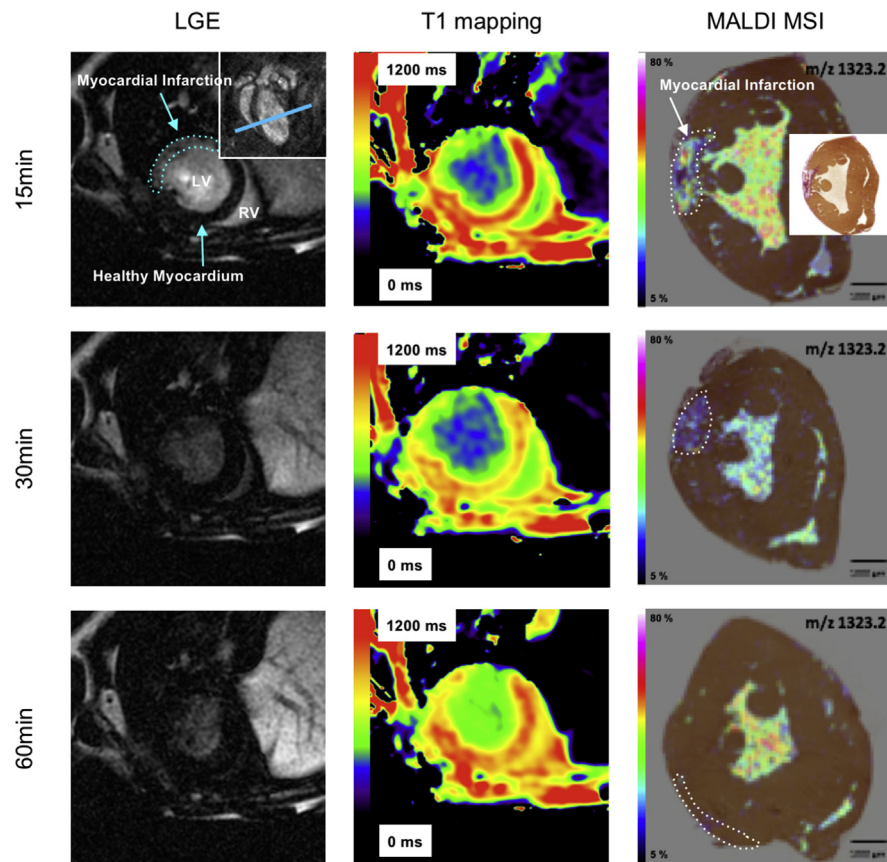


**Fig. 4.** Kinetics of Gadofluorine P by MALDI-MSI. Assessment of Gadofluorine P kinetics at 15, 30 and 60 minutes after injection in Late Gadolinium Enhancement (LGE, left column), T1 maps (middle column) and MALDI-MSI fused with Elastica-Van-Gieson staining (EvG) (right column) are shown. Right upper panel in first LGE image depicts coronal view of the heart for better anatomic orientation, blue line indicates the level of the transverse imaging planes shown in left and middle column (LV = left ventricle, LA = left atrium). Infarct delineation was based on EvG histology (small panel in first MALDI image).

after MI. In contrast  $R_1$  values of infarcted myocardium after Gadofluorine P injection were higher at 6 weeks after MI ( $2.88 \pm 0.51 \text{ s}^{-1}$ ) compared to 1 week ( $1.62 \pm 0.11 \text{ s}^{-1}$ ,  $p = 0.0422$ ). Increased  $R_1$  values at 6 weeks were corroborated by increased Gadofluorine P concentrations observed by MALDI-MSI. Gadofluorine P concentration was significantly higher ( $p = 0.0479$ ) in infarcted myocardium after 6 weeks ( $0.0283 \pm 0.0038 \text{ mM}$ ) compared to the earlier time point at 1 week post MI ( $0.0198 \pm 0.0054 \text{ mM}$ ) (Fig. 5A–C). Interestingly, direct correlation of  $R_1$  values at 1 and 6 weeks showed only a moderate correlation with the actual Gadofluorine P concentration in tissue, both for the infarct and remote myocardium (Fig. 5D and E).

### 3.4. Gadolinium tissue analysis by elemental LA-ICP-MS

While MALDI-MSI provides probe assessment of molecular MR contrast agents, LA-ICP-MS provides a fully quantitative analysis of gadolinium in tissue and

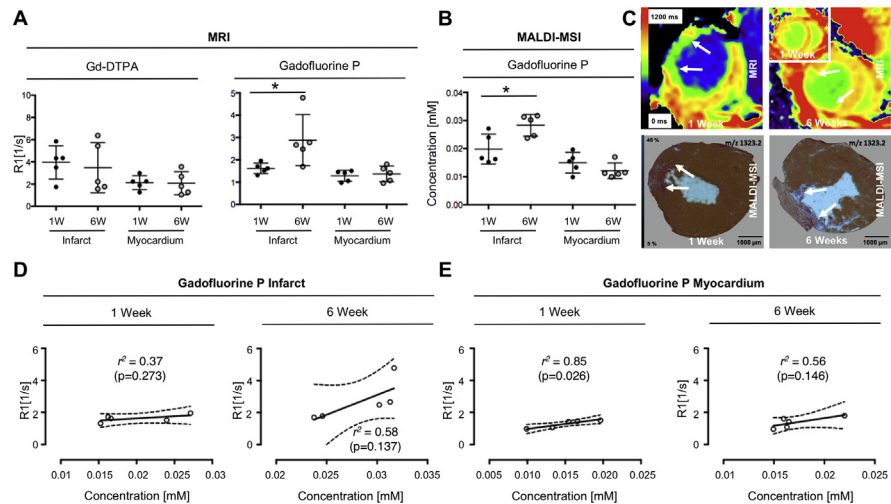


**Fig. 5.** Gadofluorine P enhancement at 1 and 6 weeks after myocardial infarction. A) Comparison of  $R_1$  values for Gd-DTPA and Gadofluorine P at 1 and 6 weeks after myocardial infarction ( $n = 5$ , scanned subsequently on week 1 and 6). While Gd-DTPA enhancement does not change between 1 and 6 weeks post MI, Gadofluorine P induces increased  $R_1$  values at 6 compared to 1 week ( $p = 0.0422$ ). B) Gadofluorine P concentration assessed by MALDI-MSI 1 and 6 weeks after myocardial infarction revealed increased Gadofluorine P uptake at 6 weeks ( $p = 0.0479$ );  $n = 5$  mice for week 1 and  $n = 5$  for week 6 (6 weeks mice same as Fig. 3A). C) Representative images of Gadofluorine P accumulation in myocardial infarction (MI) in vivo (T1 maps upper row) and ex vivo (MALDI-MSI fusion with EvG, lower row) at 1 and 6 weeks after MI. MALDI-MSI images were obtained from the same mice as the corresponding MR images. The inset T1 map (first row in the upper left corner) shows the corresponding T1 map of the same mouse obtained at 1 week compared to 6 weeks (first row large panel on the right). D) Correlation of  $R_1$  values ( $n = 5$  mice for each time point) in infarcted myocardium with Gadofluorine P concentration at 1 ( $r^2 = 0.37$ ) and 6 ( $r^2 = 0.58$ ) weeks after MI show only moderate correlations between contrast agent concentration and  $R_1$ . E) Similarly, within the healthy myocardium correlation of  $R_1$  values in healthy myocardium with Gadofluorine P concentration by MALDI-MSI at 1 ( $r^2 = 0.85$ ) and 6 weeks ( $r^2 = 0.56$ ) after MI show only moderate agreement. \* indicates  $p$ -value < 0.05.

provides improved spatial resolution compared to MALDI-MSI. Therefore, we chose to additionally analyze tissue samples by LA-ICP-MS. LA-ICP-MS provided quantification of Gd in infarcted mouse hearts at a resolution of down to  $15 \mu\text{m}$  (Fig. 6A). Confirming the results obtained by MALDI-MSI, LA-ICP-MS reveals that Gd concentrations in infarcted tissue increased at 6 weeks compared to 1 week after MI, representative for progressive scar formation (Fig. 6B). Similarly, the kinetic profile of gadolinium accumulation in tissue, both infarct and remote myocardium, corresponded to the kinetics revealed by MALDI-MSI (Fig. 6C).

### 3.5. Extracellular matrix synthesis assessment by histology

To verify the increased signal at 6 weeks gained by Gadofluorine P, ECM synthesis in the infarct scar was assessed by Elastica-Van-Gieson staining (EvG) (Fig. 7A and B).

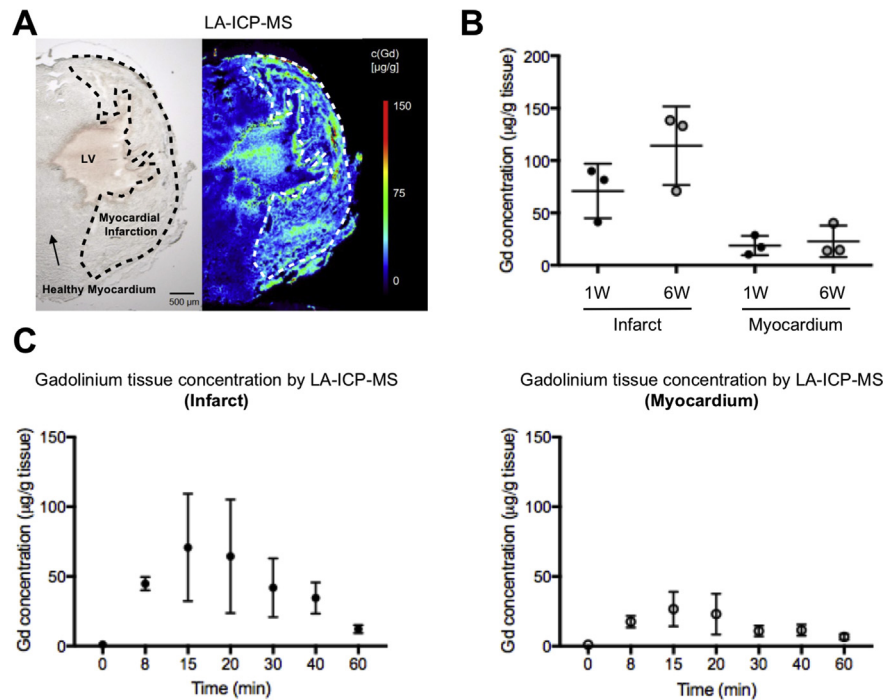


**Fig. 6.** Quantitative Gadolinium assessment by Laser Ablation – Inductively Coupled Plasma - Mass Spectrometry (LA-ICP-MS). A) Unstained microscopy image (left) and representative LA-ICP-MS image of Gd distribution of the isotope  $^{158}\text{Gd}$  in the area of myocardial infarction 15 minutes after injection with a spatial resolution/spot size, of 15 µm. (B) Dot plots show increased Gd concentration at six weeks compared to 1 week after myocardial infarction, in infarcted tissue but also to some degree in healthy myocardium ( $n = 3$  for 1 and  $n = 3$  for 6 weeks timepoint). (C) Kinetic profile of Gd accumulation in infarcted and healthy myocardium was comparable to the results obtained by MALDI-MSI with peak concentrations at 15 minutes after injection ( $n = 3$  per time point (in minutes) after Gd-injection).

The mean red chromogen intensity as well as the ratio of the red stained area/all ROI area increased significantly at 6 weeks after MI compared to the early time point at 1 week, representing an increasing ECM synthesis content during myocardial scar formation ( $p = 0.0014$  and  $p < 0.0001$ , Fig. 7C and D). Thus, the increased MRI signal for Gadofluorine P was confirmed by an increase in ECM synthesis on histology.

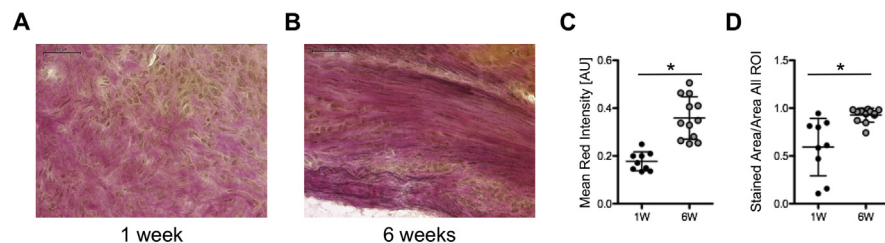


**Fig. 7.** Assessment of extracellular matrix synthesis. A) Elastica-van-Gieson staining of myocardial infarction at 1 week and B) at 6 weeks (scale bar is 50 µm). C) Comparison of Mean Red Intensity in EvG Staining of myocardial infarction after 1 ( $n = 9$ ) and 6 ( $n = 12$ ) weeks shows increase in extracellular matrix during progressive scar formation ( $p = 0.0014$ ). D) Comparison of the ratio Stained Area/Area all ROI in EvG staining of myocardial infarction after 1 ( $n = 9$ ) and 6 ( $n = 12$ ) weeks similarly shows increase of extracellular matrix at 6 weeks post MI ( $p < 0.0001$ ). \* indicates  $p$ -value  $< 0.05$ .

### 3.6. Relationship between contrast enhancement and LV function

To evaluate the relationship of ECM synthesis during scar formation and associated cardiac function, CINE imaging was additionally performed.  $R_1$  values in infarcted myocardium after the injection of Gadofluorine P as well as MALDI-MSI results for Gadofluorine P concentration were thus correlated to the left ventricular function. While there was no correlation observed between  $R_1$  values ( $r^2 = 0.01$ ,  $p = 0.901$ ) and Gadofluorine P concentration ( $r^2 = 0.19$ ,  $p = 0.466$ ) at 1 week post MI (Fig. 8A), 6 weeks after MI a positive correlation was seen between  $R_1$  values and the ejection fraction (EF) ( $r^2 = 0.65$ ,  $p = 0.097$ ). Interestingly the local Gadofluorine P concentrations at 6 weeks demonstrated an even higher correlation with the EF compared to the  $R_1$  values ( $r^2 = 0.89$ ,  $p = 0.014$ ) (Fig. 8B).

## 4. Discussion

In the current study, we establish a combined MR and MSI approach to study Gadofluorine P deposition during scar formation in a mouse model of myocardial infarction. We attribute the signal increase of Gadofluorine P to post-MI scar formation

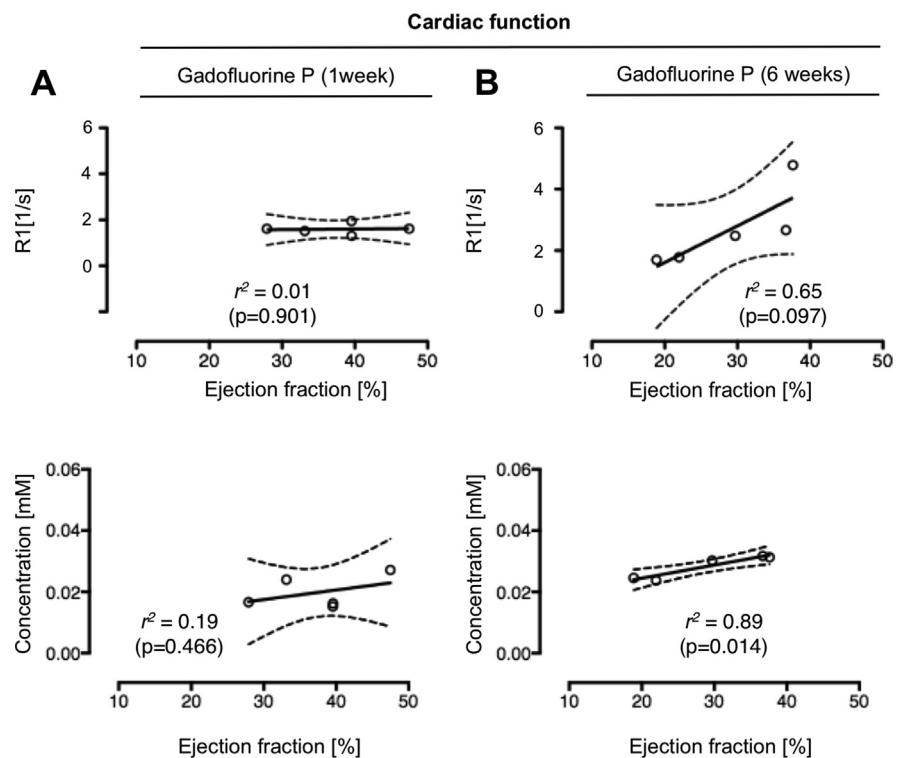


**Fig. 8.** Correlation of Gadofluorine P enhancement with left-ventricular function at 1 and 6 weeks post myocardial infarction. Correlation of  $R_1$  values (first row;  $n = 5$ ) as well as tissue concentrations of Gadofluorine P (second row) at 1 week ( $n = 5$ ) (Panel A) and 6 weeks ( $n = 5$ ) (Panel B) after MI for infarcted myocardium with the corresponding ejection fraction.

with increased ECM synthesis and show that mice with increased Gadofluorine P enhancement and tissue concentrations have a markedly improved ejection fraction at six weeks post MI. The signal increase detected *in vivo* at six weeks by MRI is accompanied by an increase in Gadofluorine P-concentration in tissue as determined by MALDI-MSI and LA-ICP-MS.

Precise quantification of the imaging signal is important to track the process of myocardial healing as well as to assess the response to therapy. Quantification of the MRI signal *in vivo* is still considered the Achilles' heel of modern MRI [17, 18]. SNR/CNR both depend on imaging parameters (e.g. inversion time, flip angle) and hardware settings (e.g. receiver gain), and thus are not quantitative. T1 mapping-approaches allow a semi-quantitative assessment of signal enhancement by calculating the T1 value for each pixel [19]. This is *semi*-quantitative because the signal observed *in vivo* depends on multiple factors of the local environment such as pH, temperature, or compartmentalization of the contrast agent. Additionally, targeted contrast agents modify their chemical structure, molecular weight and tumbling rate once bound to specific biomarkers. Thus measuring the local concentration of such a contrast agent depends both on the free and bound fraction of the contrast agent which is a challenging task *in vivo* [20]. Methods determining actual probe concentration in tissue post imaging would be valuable to better judge and improve *in vivo* imaging results.

Gadofluorine P has been developed from its precursor substance Gadofluorine M. Gadofluorine M has been shown to bind to ECM proteins such as collagen, tenascin and proteoglycans of the vessel wall in various animal models of atherosclerosis [14, 21, 22, 23, 24]. These ECM proteins can also be found in scar tissue after myocardial infarction. Here we focused on Gadofluorine P due to its favorable kinetic profile. It should be noted however that binding constants of Gadofluorine P for specific extracellular matrix components have yet to be reported, but - as an amphiphilic agent similar in structure to Gadofluorine M - it is expected to bind to proteins and filaments of the ECM due to different surface charges. Of note, we observed quite some variation of R1 values at 6 weeks post MI both for Gd-DTPA and Gadofluorine P. This may be due to a physiological variation of the healing response but also reflect the spatial heterogeneity of healing.

Healing of myocardial infarction in mice has been shown to occur in a biphasic manner [25]. After 1 week the process of myocardial remodeling is still at its beginning, while at the later time points synthesis of extracellular matrix, formation of scar tissue and restructuring of elastic fibers has already led to a significant rearrangement of the left ventricle [8, 26]. Gadofluorine P-signal intensity and tissue concentration in the infarct scar correlate with ejection fraction in the course at 6 weeks after MI, indicating that T1 mapping with MRI shows promise for correlating ECM deposition in the infarct zone with cardiac function during infarct healing.

A direct correlation analysis demonstrated only poor correlation between  $R_1$  values and Gadofluorine P tissue concentrations. This may have several reasons. First, these correlations were not performed on a pixel-by-pixel comparison. This is hardly possible as tissue preparation of the MALDI-MSI slides leads to changes in tissue shape, e.g. through drying and shrinkage. Additionally, MALDI-MSI is performed on slides with 12  $\mu\text{m}$  thickness, while the slide thickness in MRI was 1mm. Therefore, ROI-based analysis has to be performed. But more importantly, the only moderate correlations demonstrate the weakness of *in vivo* MRI: the insufficiency to provide quantitative molecular imaging data. Different biological as well as chemical surroundings of the probe significantly affect the signal *in vivo*, leading to reduction in correlation between the measured MRI signal and the actual concentration of the contrast agent. These confounders are unavoidable and emphasize the need to bridge the gap towards quantification, which we show to be feasible by MSI. Niehoff et al. recently proposed to calculate a conversion function from  $R_1$  and concentration values and to subsequently determine *in vivo* contrast agent concentration maps from T1 maps mathematically [27]. Based on the correlation of data obtained by MRI and Mass Spectrometry Imaging, the calibration of contrast-enhanced MRI experiments by spatially resolved mass spectrometry imaging is possible.

Additionally, MSI has superior resolution as compared to MRI: currently MALDI-MSI can reach a resolution of up to 30 $\mu\text{m}$ , and laser ablation-inductively coupled plasma-mass spectrometry (LA-ICP-MS) can provide gadolinium distribution maps at a resolution of 15  $\mu\text{m}$  [28, 29]. This resolution – approaching cellular levels - potentially allows for more profound evaluation of target structures of molecular and cellular gadolinium agents. With the advent of MSI, one can now match the accumulation of specific contrast agents spatially to their cellular and molecular surroundings.

The study has several limitations: 1) Exact co-registration of MRI T1 maps and gadolinium distribution maps has not been possible due to the experimental setup, different slice thicknesses and voxel size. 2) Although a promising technology, MALDI-MSI has the drawback that on the one hand the signal is dependent on the overlying matrix. On the other hand, the spatial resolution of MALDI-MSI does not reach the cellular range. LA-ICP-MS, as additionally shown, is based on elemental mass spectrometry imaging detecting total Gd in tissue, shows only little matrix dependency and provides accurate, spatially resolved quantitative data. Additionally, LA-ICP-MS can reach a resolution of down to 5 microns, so that LA-ICP-MS might become a valuable complementary method to MALDI-MSI. 3) Gadofluorine P creates higher  $R_1$  values in the blood compared to the infarct region, which is not optimal for molecular MRI of cardiac tissue. 4) The small sample size of this experimental pilot study allows only for preliminary conclusions. Especially experiments correlating contrast agent concentration to signal enhancement will have to be performed in larger cohorts.

In summary, we demonstrate the feasibility to validate T1 mapping by ex vivo Mass Spectrometry Imaging. MSI enables to quantify the accumulation of Gadofluorine P directed towards extracellular matrix proteins during myocardial scar formation. Quantitative values of gadolinium in tissue provided at high spatial resolution is beneficial for validation of in vivo molecular imaging and development of future imaging biomarkers.

## Declarations

### Author contribution statement

Fabian Lohöfer: Conceived and designed the experiments; Performed the experiments; Analyzed and interpreted the data; Wrote the paper.

Laura Hoffmann: Performed the experiments; Analyzed and interpreted the data.

Rebecca Buchholz: Performed the experiments; Analyzed and interpreted the data; Contributed reagents, materials, analysis tools or data.

Katharina Huber, Almut Glinzer: Performed the experiments.

Katja Kosanke, Annette Feuchtinger, Michaela Aichler, Georgios Kaissis, Franz Schilling: Analyzed and interpreted the data.

Benedikt Feuerecker, Carsten Höltke: Analyzed and interpreted the data; Contributed reagents, materials, analysis tools or data.

Ernst Rummeny: Conceived and designed the experiments.

Cornelius Faber, Axel K. Walch, Uwe Karst: Analyzed and interpreted the data; Contributed reagents, materials, analysis tools or data; Wrote the paper.

René Btonar: Conceived and designed the experiments; Wrote the paper.

Moritz Wildgruber: Conceived and designed the experiments; Analyzed and interpreted the data; Contributed reagents, materials, analysis tools or data; Wrote the paper.

### Funding statement

This work was supported by a Deutsche Forschungsgemeinschaft grant WI3686/4-1 to MW, and the Core Unit PIX of the Interdisciplinary Center for Clinical Research, Münster University Hospital.

### Competing interest statement

The authors declare no conflict of interest.



## Additional information

No additional information is available for this paper.

## References

- [1] C.A. Souders, S.L. Bowers, T.A. Baudino, Cardiac fibroblast: the renaissance cell, *Circ. Res.* 105 (12) (2009) 1164–1176.
- [2] N.G. Frangogiannis, The extracellular matrix in myocardial injury, repair, and remodeling, *J. Clin. Invest.* 127 (5) (2017) 1600–1612.
- [3] M.A. Konstam, D.G. Kramer, A.R. Patel, M.S. Maron, J.E. Udelson, Left ventricular remodeling in heart failure: current concepts in clinical significance and assessment, *JACC Cardiovasc. Imaging* 4 (1) (2011) 98–108.
- [4] Y. Ma, G.V. Halade, M.L. Lindsey, Extracellular matrix and fibroblast communication following myocardial infarction, *J. Cardiovasc. Transl. Res.* 5 (6) (2012) 848–857.
- [5] Y. Ma, A. Yabluchanskiy, M.L. Lindsey, Neutrophil roles in left ventricular remodeling following myocardial infarction, *Fibrogenesis Tissue Repair* 6 (1) (2013) 11.
- [6] P.A. Helm, P. Caravan, B.A. French, et al., Postinfarction myocardial scarring in mice: molecular MR imaging with use of a collagen-targeting contrast agent, *Radiology* 247 (3) (2008) 788–796.
- [7] P. Caravan, B. Das, S. Dumas, et al., Collagen-targeted MRI contrast agent for molecular imaging of fibrosis, *Angew. Chem.* 46 (43) (2007) 8171–8173.
- [8] M. Wildgruber, I. Bielicki, M. Aichler, et al., Assessment of myocardial infarction and postinfarction scar remodeling with an elastin-specific magnetic resonance agent, *Circ. Cardiovasc. Imaging* 7 (2) (2014) 321–329.
- [9] J. Baxa, J. Ferda, M. Hromadka, T1 mapping of the ischemic myocardium: review of potential clinical use, *Eur. J. Radiol.* 85 (10) (2016) 1922–1928.
- [10] A. Tanimoto, K. Oshio, M. Suematsu, D. Pouliquen, D.D. Stark, Relaxation effects of clustered particles, *J. Magn. Reson. Imaging* 14 (1) (2001) 72–77.
- [11] E. Terreno, S. Geninatti Crich, S. Belfiore, et al., Effect of the intracellular localization of a Gd-based imaging probe on the relaxation enhancement of water protons, *Magn. Reson. Med.* 55 (3) (2006) 491–497.
- [12] M. Aichler, K. Huber, F. Schilling, et al., Spatially resolved quantification of gadolinium(III)-based magnetic resonance agents in tissue by MALDI

- imaging mass spectrometry after in vivo MRI, *Angew Chem. Int. Ed. Engl.* 54 (14) (2015) 4279–4283.
- [13] M. Birka, K.S. Wentker, E. Lusmoller, et al., Diagnosis of nephrogenic systemic fibrosis by means of elemental bioimaging and speciation analysis, *Anal. Chem.* 87 (6) (2015) 3321–3328.
- [14] J. Meding, M. Urich, K. Licha, et al., Magnetic resonance imaging of atherosclerosis by targeting extracellular matrix deposition with Gadofluorine M, *Contrast Media Mol. Imaging* 2 (3) (2007) 120–129.
- [15] D.R. Messroghli, A. Rudolph, H. Abdel-Aty, et al., An open-source software tool for the generation of relaxation time maps in magnetic resonance imaging, *BMC Med. Imaging* 10 (2010) 16.
- [16] R. Deichmann, D. Hahn, A. Haase, Fast T1 mapping on a whole-body scanner, *Magn. Reson. Med.* 42 (1) (1999) 206–209.
- [17] D. Radenkovic, S. Weingartner, L. Ricketts, J.C. Moon, G. Captur, T1 mapping in cardiac MRI, *Heart Fail. Rev.* 22 (4) (2017) 415–430.
- [18] B.F. Coolen, C. Calcagno, P. van Ooij, Z.A. Fayad, G.J. Strijkers, A.J. Nederveen, Vessel wall characterization using quantitative MRI: what's in a number? *MAGMA* 31 (1) (2018) 201–222.
- [19] D.O. h-Ici, S. Jeuthe, N. Al-Wakeel, et al., T1 mapping in ischaemic heart disease, *Eur. Heart J. Cardiovasc. Imaging* 15 (6) (2014) 597–602.
- [20] L.A. Ekanger, M.J. Allen, Overcoming the concentration-dependence of responsive probes for magnetic resonance imaging, *Metalomics* 7 (3) (2015) 405–421.
- [21] J. Barkhausen, Detection of atherosclerotic plaque with gadofluorine-enhanced magnetic resonance imaging, *Circulation* 108 (5) (2003) 605–609.
- [22] I. Koktzoglou, K.R. Harris, R. Tang, et al., Gadofluorine-enhanced magnetic resonance imaging of carotid atherosclerosis in Yucatan miniswine, *Invest. Radiol.* 41 (3) (2006) 299–304.
- [23] J. Zheng, E. Ochoa, B. Misselwitz, et al., Targeted contrast agent helps to monitor advanced plaque during progression: a magnetic resonance imaging study in rabbits, *Invest. Radiol.* 43 (1) (2008) 49–55.
- [24] J.A. Ronald, Y. Chen, A.J. Belisle, et al., Comparison of gadofluorine-M and Gd-DTPA for noninvasive staging of atherosclerotic plaque stability using MRI, *Circ. Cardiovasc. Imaging* 2 (3) (2009) 226–234.

- [25] M. Nahrendorf, F.K. Swirski, E. Aikawa, et al., The healing myocardium sequentially mobilizes two monocyte subsets with divergent and complementary functions, *J. Exp. Med.* 204 (12) (2007) 3037–3047.
- [26] A. Protti, B. Lavin, X. Dong, et al., Assessment of myocardial remodeling using an elastin/tropoelastin specific agent with high field magnetic resonance imaging (MRI), *J. Am. Heart Assoc.* 4 (8) (2015) e001851.
- [27] A.C. Niehoff, L. Wachsmuth, F. Schmid, M. Sperling, C. Faber, U. Karst, Quantification of manganese enhanced magnetic resonance imaging based on spatially resolved elemental mass spectrometry, *ChemistrySelect* 1 (2) (2016) 264–266.
- [28] R. Schmidt, N. Nippe, K. Strobel, et al., Highly shifted proton MR imaging: cell tracking by using direct detection of paramagnetic compounds, *Radiology* 272 (3) (2014) 785–795.
- [29] O. Reifschneider, K.S. Wentker, K. Strobel, et al., Elemental bioimaging of thulium in mouse tissues by laser ablation-ICPMS as a complementary method to heteronuclear proton magnetic resonance imaging for cell tracking experiments, *Anal. Chem.* 87 (8) (2015) 4225–4230.